

# Supporting Information

## Superhydrophobic Asymmetric pH-responsive Soft Actuators: Implications for the Development of Anti-fouling Medical Devices

Amit Kumar<sup>a,c</sup>, Smruti Parimita<sup>b</sup>, Kumari Kiran<sup>a</sup>, Nitish R. Mahapatra<sup>a</sup>, and Pijush Ghosh<sup>c,d\*</sup>

<sup>a</sup> Department of Biotechnology, Bhupat and Jyoti Mehta School of Biosciences, Indian Institute of Technology Madras, Chennai, 600036, India

<sup>b</sup> Manufacturing Engineering Section, Department of Mechanical Engineering, IIT Madras, Chennai-600036, India

<sup>c</sup> Department of Applied Mechanics and Biomedical Engineering, Indian Institute of Technology Madras, Chennai, 600036, India

<sup>d</sup> Center for Responsive Soft Matter, Indian Institute of Technology Madras, Chennai 600036, India

\*corresponding author email: [pijush@iitm.ac.in](mailto:pijush@iitm.ac.in)

### 1. Images of prepared chitosan solution to obtain asymmetric film

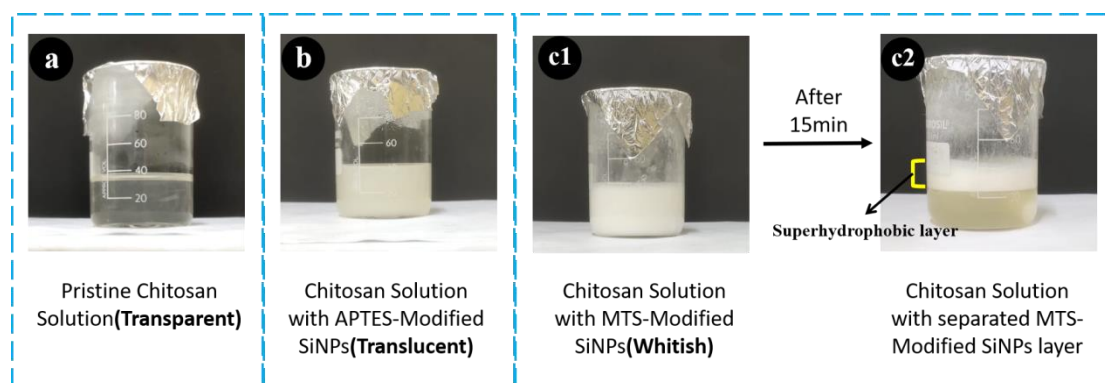


Fig. S1. Snapshot of images captured after solution preparation, (a) pristine chitosan solution, (b) chitosan solution with APTES-modified SiNPs (Hydrophilic), (c1) chitosan solution with MTS-modified SiNPs (superhydrophobic), (c2) separated layer formation of superhydrophobic SiNPs when the solution is kept undisturbed for 15 mins.

## 2. SEM attained for different sample volume and modified SiO<sub>2</sub> concentration

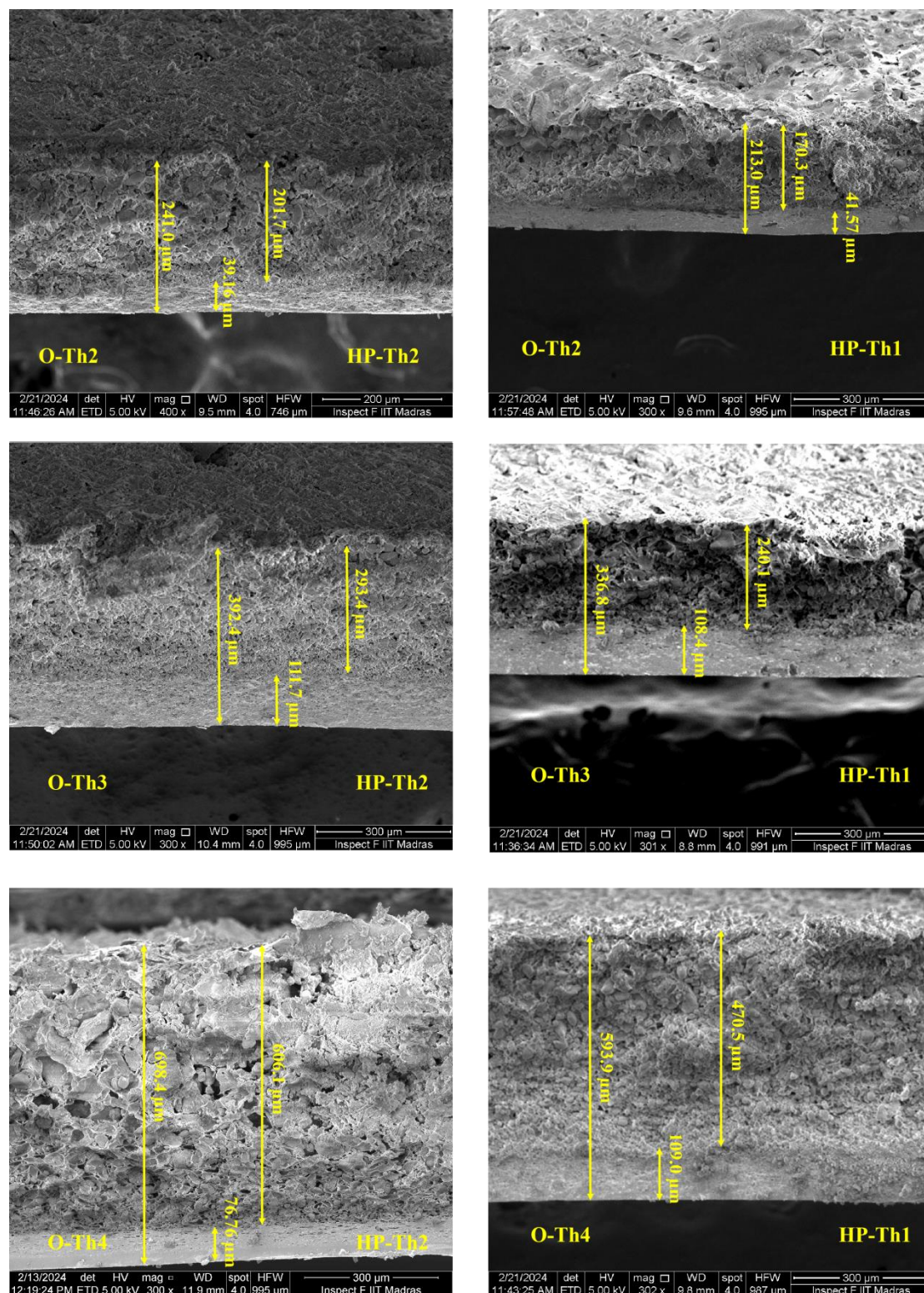


Fig. S2. SEM images indicating increase in overall thickness of O-Th2, O-Th3 and O-Th4 with increase in volume to 20ml, 30ml and 40ml respectively (vertically downward) and decrease in superhydrophobic (top) layer as concentration of SiNPs is changed from 1:1 to 1:2 (SiNPs:chitosan) (by wt) (horizontally towards right side).

### 3. SEM attained for pH responsive films

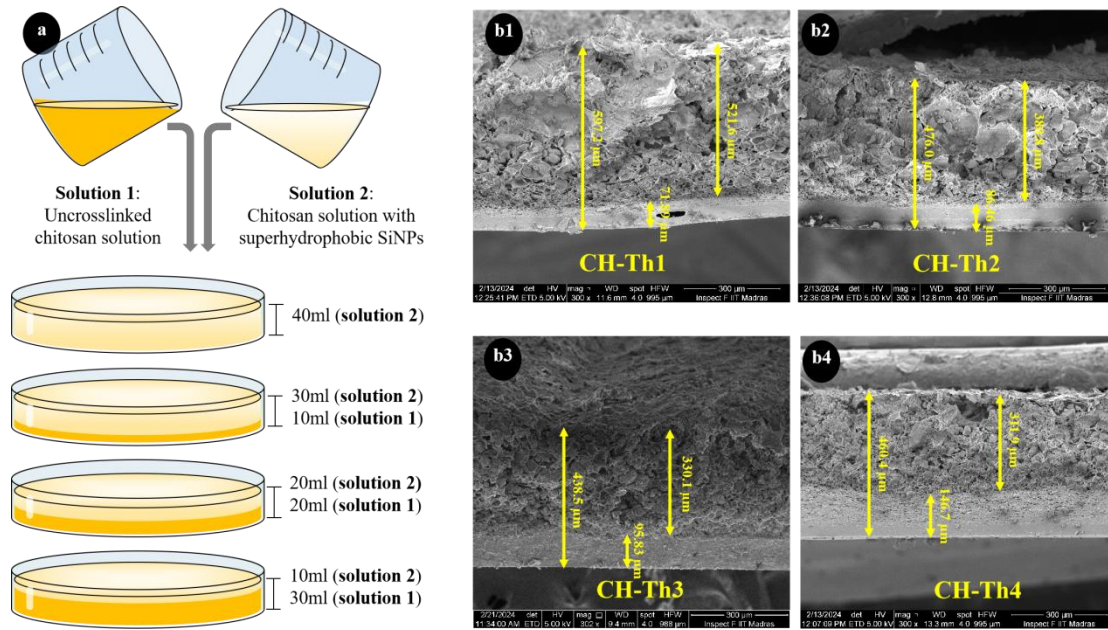


Fig. S3. (a) Schematic representation of preparation of asymmetric films to obtain different chitosan(bottom) layer thickness, (b1-b4)SEM images of prepared asymmetric film with increased bottom layer thickness with increasing the volume of chitosan solution.

### 4. Swelling Ratios of Asymmetric Chitosan Film

The swelling ratio of asymmetric chitosan film(CH-Th4) was measured in DI water, 0.1 M HCl and 0.1 M NaOH solution. The initial dimensions of the films were (1cm x1cm).

The swelling ratio (SR) was calculated as  $SR = \frac{W_s - W_d}{W_s} \times 100\%$

Where  $W_s$  and  $W_d$  respectively denote the films' swollen weight and dry weight, and an average of five measurements was reported.

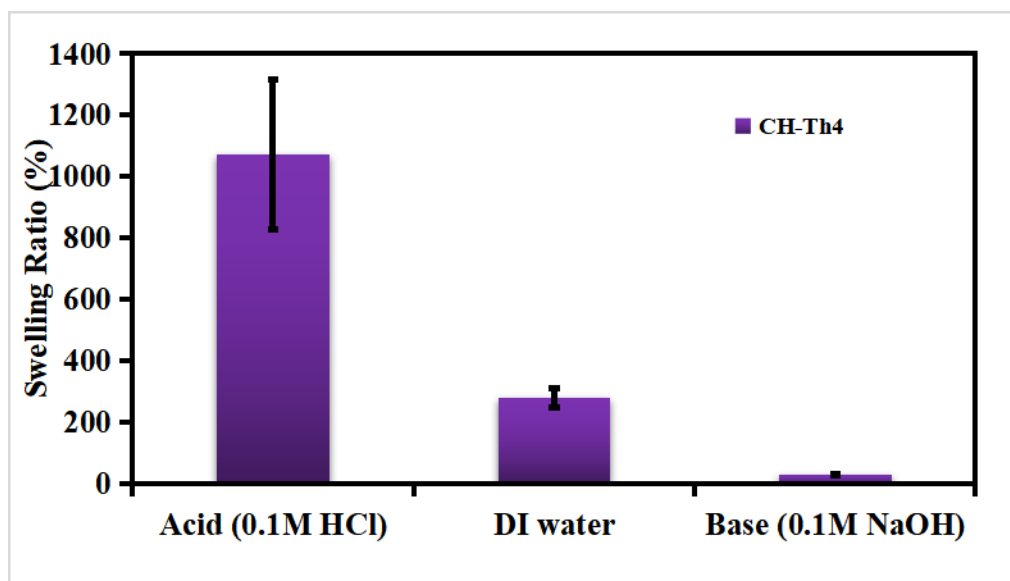


Fig. S4. Plot representing swelling ratio obtained for CH-Th4 film which showed bidirectional actuation in acidic and basic pH.

## 5. FTIR

The determination of the chemical composition of the synthesized modified silica nanoparticles surface was carried out using FTIR spectroscopy in order to confirm the modification fact. The interpretation and analysis of the IR spectra were performed on the basis of the available literature data.

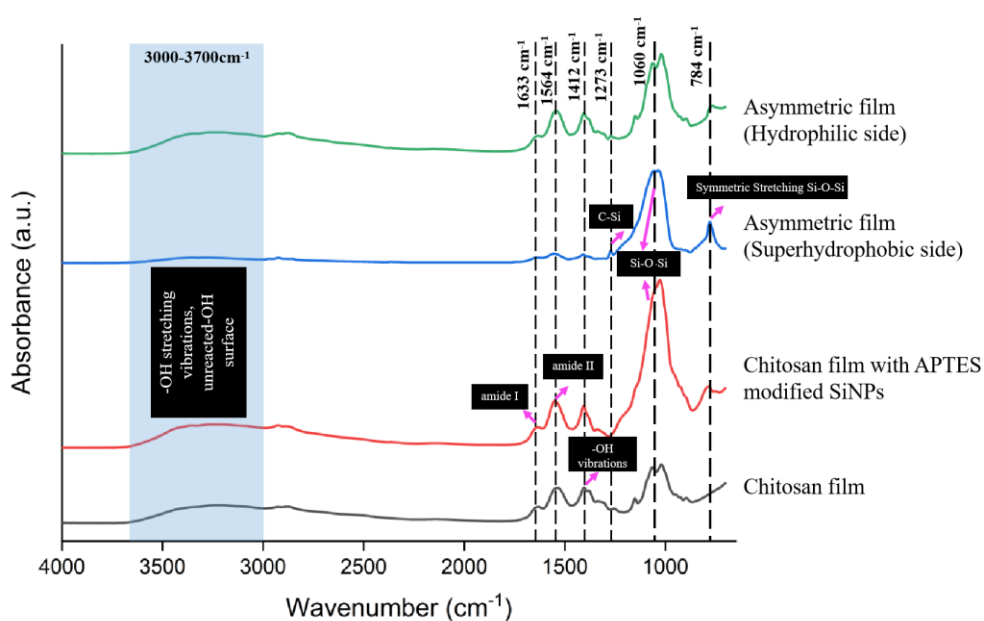


Fig. S5. FTIR plot of asymmetric film with superhydrophobic SiNPs(top and bottom surface), chitosan film with APTES modified SiNPs and pristine chitosan film



The pristine chitosan film's peaks were identified at  $1411\text{cm}^{-1}$ , indicating vibration of -OH groups,  $1564\text{cm}^{-1}$ , indicating amide II peaks, and  $1633\text{cm}^{-1}$ , indicating amide I peaks. For the chitosan film with APTES-modified SiNPs, the intensity of the peak at  $1060\text{cm}^{-1}$  increased, indicating Si-O-Si interaction. The presence of the  $\text{-NH}_2$  bend and  $\text{NH}_3^+$  bend is confirmed via peaks at  $1564\text{cm}^{-1}$  and  $1633\text{cm}^{-1}$ , respectively.

The absorbance peaks were obtained for asymmetric chitosan films with the top (superhydrophobic surface) and bottom (hydrophilic surface) sides separately. The bottom side showed similar peaks as chitosan film, indicating the superhydrophobic silica particles are diffused to the top side. However, there are indications of some unmodified SiNPs in the bottom, as confirmed by the peak at  $784\text{cm}^{-1}$  and increased peak intensity at  $1060\text{cm}^{-1}$ . For the top(superhydrophobic) side, the peak at  $1273\text{cm}^{-1}$  indicates the C-Si asymmetric stretching, which confirms the MTS-modified SiNPs. The intensity of peaks at  $1411\text{cm}^{-1}$ ,  $1564\text{cm}^{-1}$ , and  $1633\text{cm}^{-1}$  and in the  $3000\text{-}3700\text{cm}^{-1}$  range was significantly reduced, which further confirms the lack of -OH,  $\text{NH}_2$  groups.

## *6. 3D printing of asymmetric structures*

### *6.1. Preparation of printable ink*

Chitosan ink was prepared by dissolving 8% (w/v) of chitosan powder in an acidic mixture (2% v/v acetic acid, 5% v/v lactic acid, and the rest was DI water). Citric acid powder equal to the weight of chitosan powder was added to the solution to obtain highly crosslinked samples. Similarly, 4% chitosan powder and 8% SiNPs were added to the acidic mixture solution to prepare SiNPs-CS ink. Both the solutions were kept at rest for 12 hrs and then mechanically stirred at 200 RPM for 2 hrs to dissolve the chitosan and Si particles homogeneously and centrifuged at 3000 RPM for 1 hr to remove air bubbles.

### *6.2. Study the printability of ink*

The chitosan and SiNPs-chitosan ink was characterized using a rotational rheometer (MCR301, Anton Paar, Austria) using a 25 mm parallel plate with a measurement gap of 0.55mm. The shear thinning property, amplitude sweep, and thixotropic characterization were performed at room temperature (the working temperature of the 3D printer). To study the shear-thinning property, the viscosity of the tested hydrogel ink was measured at shear rates ranging from  $0.1$  to  $1000\text{ sec}^{-1}$ . Strain sweeps from

0.1% to 1000% at a frequency of 1 Hz were performed to determine the linear viscoelastic region (LVR). A constant strain with an LVR of 1% was chosen for the angular frequency sweeps at a range of 1–100 rad/sec. The recoverability of the chitosan and SiNPs-chitosan ink was correlated to the thixotropic behavior, and the test was performed in three steps. During the first step, a shear rate of  $0.1 \text{ sec}^{-1}$  was applied to the hydrogels for 60 sec. This corresponds to the hydrogel preparatory stage prior to printing. The second step involves the instantaneous application of a high shear rate,  $500 \text{ sec}^{-1}$  application of high shear rate,  $500 \text{ sec}^{-1}$  that was held for 10 sec. This signifies the state of hydrogel under shear force during printing. In the final step, the shear rate was reduced to its initial  $0.1 \text{ sec}^{-1}$  and they retained for 120 sec to observe the recovery of viscosity that correlates with the material behavior post-printing. The rheological measurements were carried out in order to fully characterize the gels and to relate their properties with the DIW 3D printing process.

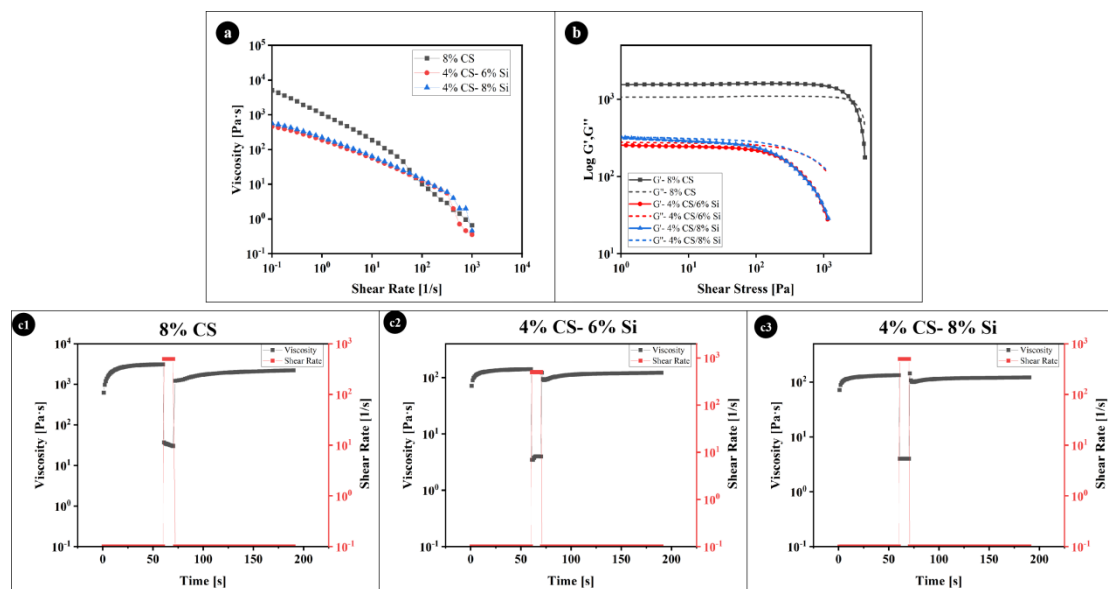


Fig. S6. Plot showing rheological characterization of chitosan and chitosan with SiNPs ink at room temperature: (a) shear viscosity as a function of shear rate, (b) storage modulus ( $G'$ ) and loss modulus ( $G''$ ) as a function of shear stress, (c1-c3) Thixotropic property

### 6.3. 3D printing of self-assembled structures

A custom-built 3D printer was fabricated in the lab with a flatbed and a rotary mandrel bed arrangement. The 3D printer works on the principle of direct-ink writing (DIW) mechanism. The printable ink was loaded into a 30ml syringe and mounted with the dispensing adaptor on the printer head, which translates in X- and Z-directions. The material was fed on a bed using compressed air pressure with a fluid

dispensing controller (supplied by Flovell Dispensers and Systems, Maharashtra, India). A flatbed was used to print planar samples, whereas a rotary mandrel was used to print 3D structures. The 3D printer was controlled by a computer through a user interface on the printer. The CAD models for 3D printing were designed using 'SolidWorks' and were converted to '.stl' format for further pre-processing. The '.stl' files were imported into an open-source slicing software, 'Ultimaker Cura,' and sliced into multiple layers based on the input parameters, namely layer thickness, printing speed, infill density, and infill pattern. The chitosan structures were printed onto the acrylic substrate with the optimized printing parameters listed in the table. The printed structures were dried under vacuum at 50° C for 24-48hrs and cured at 150° C for 10 min to cross-link the samples.

Printing parameters	Chitosan ink	SiNPs-chitosan ink
Nozzle dia(mm)	0.5	0.3
Printing pressure(bar)	5	2
Printing speed(mm/sec)	5	5

#### 7. *Mechanical characterisation of Asymmetric films*

The mechanical characterisation of pristine chitosan and asymmetric film was done. A tensile test was performed at 1 kN load and 1 mm/min displacement. A flexural test was performed with asymmetric film (1.2 mm thickness, 45 mm length and 13 mm width) and pristine chitosan (0.1 mm thickness, 45 mm length and 13 mm width) using a three-point bending setup in Universal Tensile Machine with a crosshead speed of 1 mm/min. All the experiments were repeated at least 3 times. The following are some of the results that we obtained.

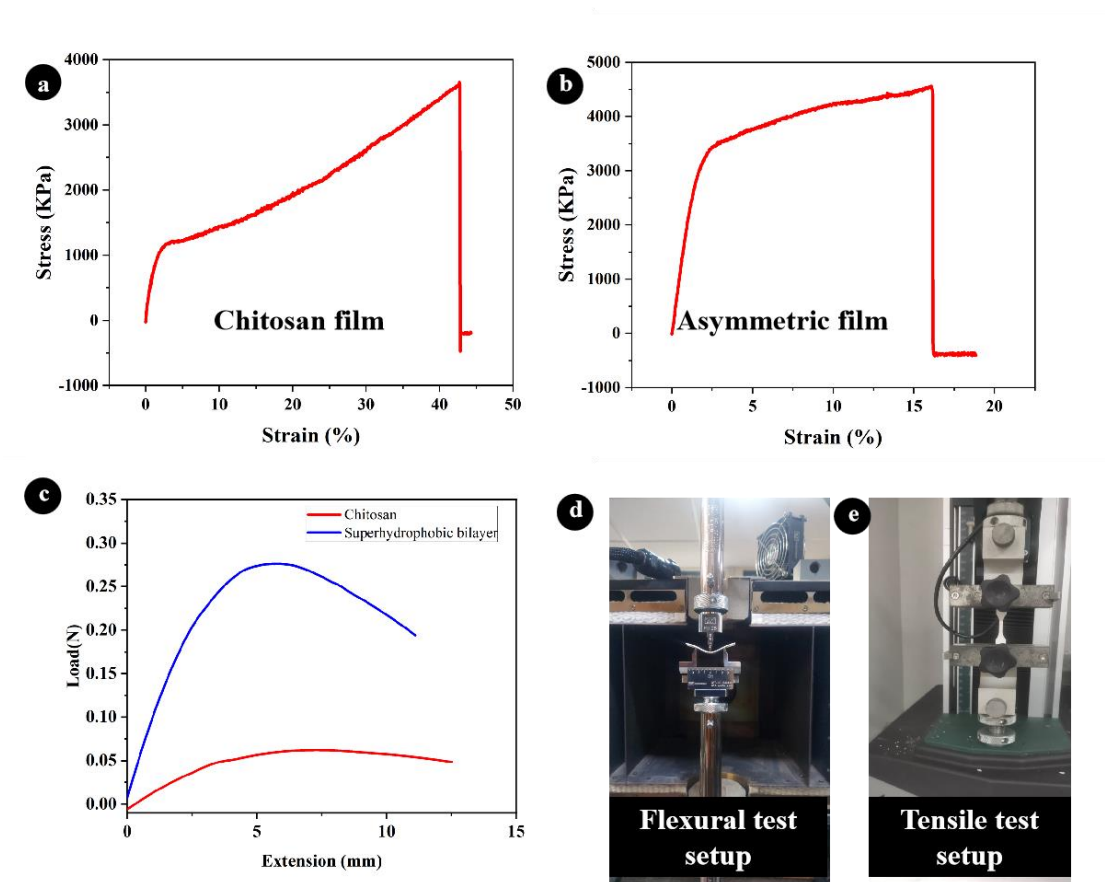


Fig. S7. (a,b) Tensile test results of chitosan film and asymmetric film, (c) Flexural test results, (d,e) photographs of flexural test and tensile test setup

The Young's modulus of chitosan film and asymmetric film obtained from the tensile test are 551.09 KPa and 2.01 MPa, respectively. As observed from the above plot, the tensile strength of both films looks similar. However, strain to failure is shown to be much lesser for the asymmetric film.

The bending modulus obtained from the flexural (3-point bending) test was 0.00329 MPa for pristine chitosan and 0.092 MPa for asymmetric film, indicating the asymmetric film has high bending strength.

#### 8. *Quantitative Antibacterial analysis of Asymmetric films*

Quantitative tests have been performed using serial dilution for colony count, and OD600 for absorbance measurements.



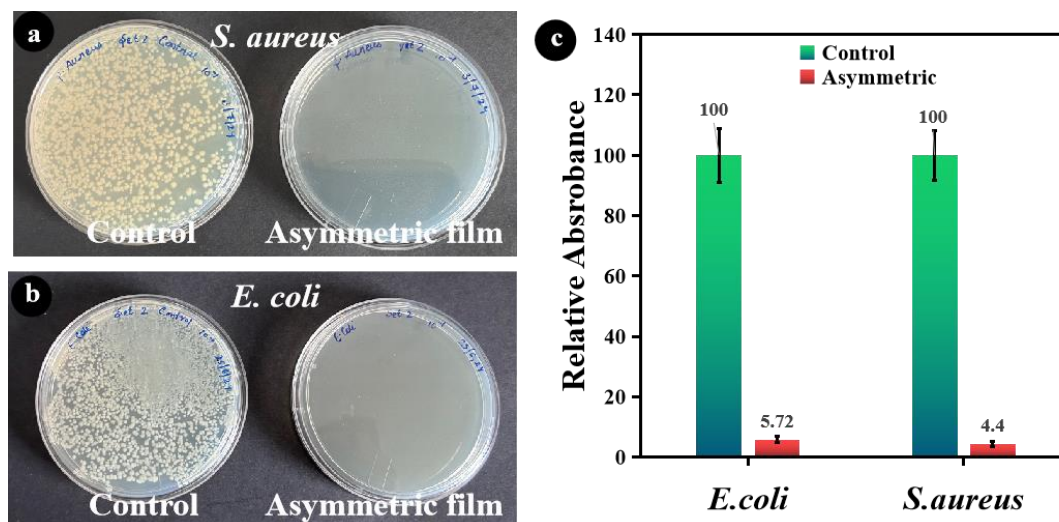


Fig. S8. (a,b) Photographs of *E. coli* colonies formed on agar plates with different dilution multiple after 18 hrs incubation. (c) For quantitative measurement, 1 ml of bacterium suspension was withdrawn, and an absorbance value at 600 nm was recorded. The relative values were calculated with respect to the absorbance value of the *E. coli* and *S. aureus* bacterium suspension transferred from asymmetric film (sample) and chitosan film(control) washed to cultured medium (absorbance = 1.22 (*E. coli*) and 3.24 (*S. aureus*))

As shown in Fig. S8. (a,b), the *E. coli* and *S. aureus* colonies detached from the pristine chitosan (control) surface were densely and evenly distributed on the surface of the agar plate, showing poor antibacterial ability. In contrast, no colonies of *E. coli* and *S. aureus* were found on the agar plate surfaces, especially in the 10-fold dilution plate, demonstrating that the asymmetric film with a superhydrophobic surface exhibited excellent antibacterial properties with 100 % antibacterial efficiency.

The absorbance values at 600 nm Fig. S8. (c) of bacterial suspension cultured in the presence of various surfaces provide a quantitative value of bactericidal activity. The relative absorbance of *E. coli* and *S. aureus* on asymmetric films was found to be 5.72 % and 4.4 %, indicating superior antifouling properties (as compared to the control conditions).

## 9. Transmission Electron Microscopy(TEM) Analysis

Transmission electron microscopy (TEM), energy dispersive X-ray spectroscopy (EDS) spectrum and electron diffraction pattern were obtained from the JEOL F200 instrument. Fig. S9. (a1) and Fig. S9. (a2) are the TEM images of unmodified and superhydrophobic silica nanoparticles, respectively. The TEM image clearly shows

particle agglomeration for both modified and unmodified silica nanoparticles at 100 nm with particle size ranging from 10-20 nm.

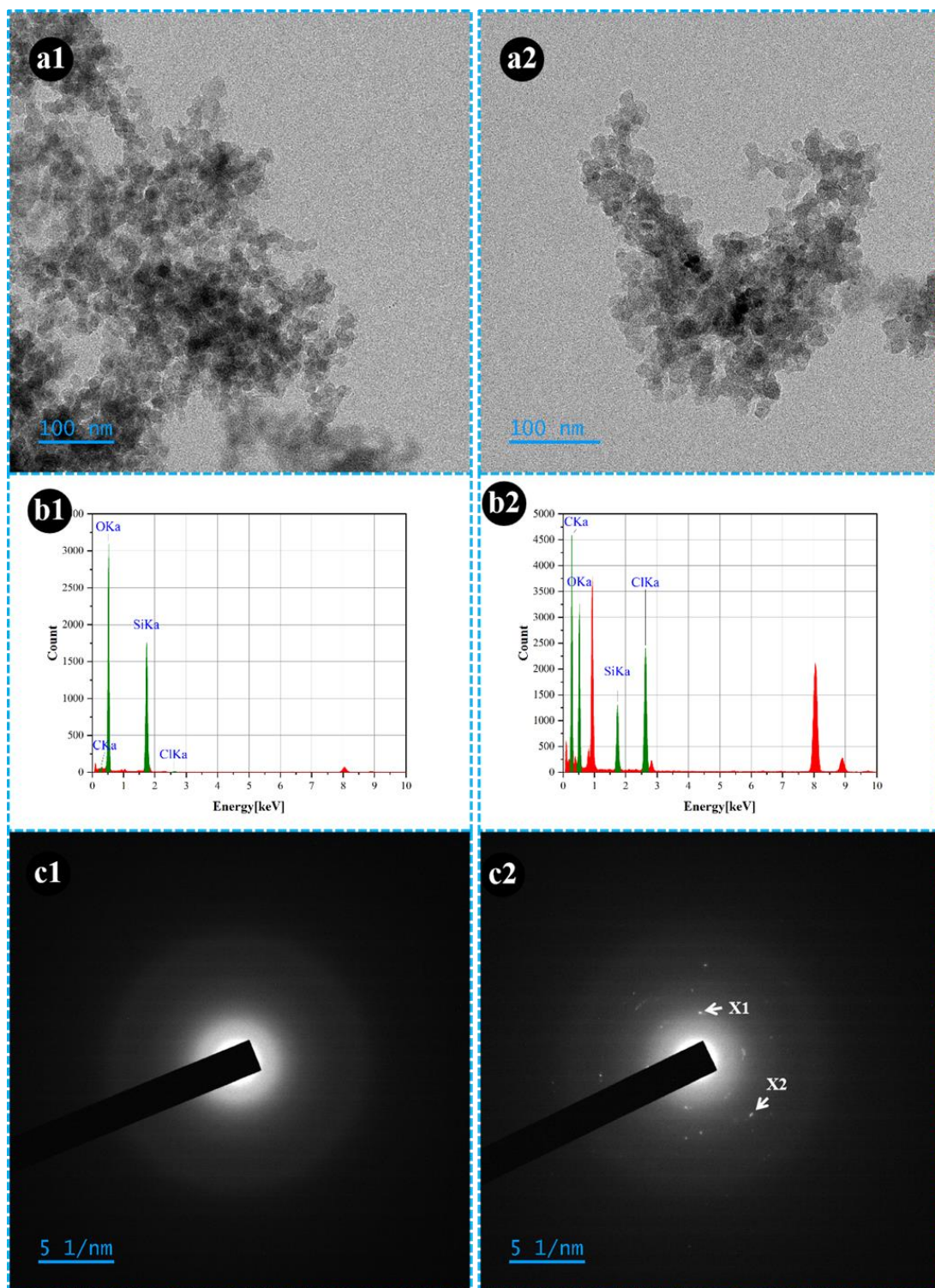


Fig. S9. (a1, a2) TEM images at 100nm, (b1, b2) EDS spectrum and (c1, c2) Electron diffraction image of superhydrophobic SiNPs and unmodified SiNPs.

The chemical composition of the unmodified and modified silica nanoparticles was analysed by an EDS spectrum (Fig. S9. (b1) and Fig. S9. (b2)), which shows that the

unmodified SiNPs consist of only Si and O peaks, whereas MTS-modified SiNPs show C and Cl peaks along with Si and O peaks, hence confirming the chemical modification of SiNPs. The features marked here X1, X2 in Fig. S9. (c2) are an indication of the crystalline nature of MTS-modified SiNPs from the electron diffraction analysis.